

April 2022

## Capacity Estimation Of Lithium Ion Battery To Evaluate SOH Using Machine Learning Method

Shravan Basvaraj B Mr.

*M S Ramaiah Institute of Technology*, shravanbb148@gmail.com

Kusumika Krori Dutta Mrs

*M S Ramaiah Institute of Technology*, kusumikadebkrori@gmail.com

Follow this and additional works at: <https://www.interscience.in/ijess>



Part of the [Electrical and Electronics Commons](#)

---

### Recommended Citation

B, Shravan Basvaraj Mr. and Krori Dutta, Kusumika Mrs (2022) "Capacity Estimation Of Lithium Ion Battery To Evaluate SOH Using Machine Learning Method," *International Journal of Electronics Signals and Systems*: Vol. 4: Iss. 3, Article 4.

DOI: 10.47893/IJESS.2022.1215

Available at: <https://www.interscience.in/ijess/vol4/iss3/4>

This Article is brought to you for free and open access by the Interscience Journals at Interscience Research Network. It has been accepted for inclusion in International Journal of Electronics Signals and Systems by an authorized editor of Interscience Research Network. For more information, please contact [sritampatnaik@gmail.com](mailto:sritampatnaik@gmail.com).

# Capacity Estimation Of Lithium Ion Battery To Evaluate SOH Using Machine Learning Method

<sup>1</sup>Shravan Basvaraj B, <sup>2</sup>Kusumika Krori Dutta

<sup>1,2</sup>M S Ramaiah Institute of Technology

**Abstract-**Electric Vehicles (EVs) are becoming more and more financially viable as the operating costs of EVs fall dramatically in comparison to Internal Combustion Engine Vehicles (ICEVs). To boost consumer trust in EVs even further, accurate State of Health - SOH measurement is essential. SOH in a battery is determined by a number of parameters, including current, voltage, age, and temperature. Estimating the SOH of a Lithium-ion battery chemistry is of a difficult task. Because lithium-ion batteries are extremely nonlinear, time-variant, and complicated electrochemical systems, this is the case. Two machine learning techniques are used to estimate SOH from Lithium-ion battery cell experimental test data. Experiments are carried out using data from NASA's Prognostic Center of Excellence.

**Key words-** State Of Health(SOH), Electric Vehicle(EV), Battery Management System(BMS)

## I. INTRODUCTION

Because of the high power and energy, lithium-ion batteries are a major component in electric vehicles (EVs), electric gadgets, storage devices, and smart electric grids[1]. Lithion batteries therefore are extensively used in a variety of areas due to their properties of extended life cyclers', high energy, less self discharge rate quality, range of temperature it works, and low environmental contamination.

To maintain safety and dependability, a battery management system (BMS) is required. The chemical and physical characteristic of battery, on the other hand always change throughout the storage and usage, which results in a reduction in power and capacity off battery. One of the most pressing issues for battery systems is the state-of-health (SOH) assessment of lithion batteries (LIBs), particularly in large-scale applications like electric automobiles and grid storage systems. LIBs lose capacity, resistance increases, and voltage decline as they age, making battery management more challenging during repeated charging and usage. Accurate battery diagnosis will aid in the modification of charging procedures to minimize misuse or even thermal runaway. [2].

There are two types of methodologies for estimating SOH: model-based methods and data-driven methods[3][4]. equivalent model of circuit, model

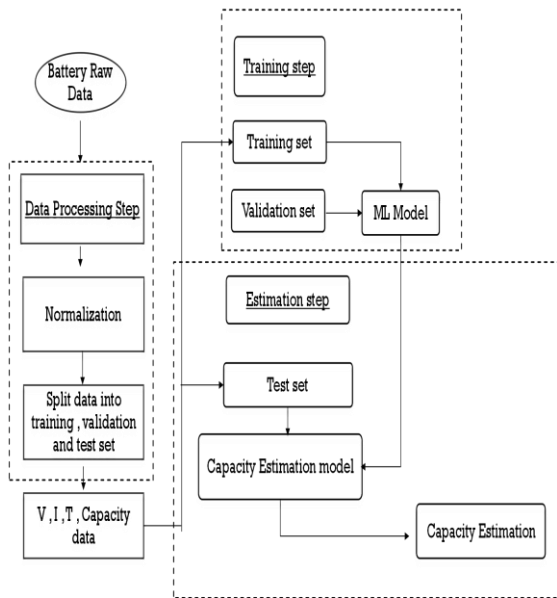
based like electrochemical, and semi empirical approach model based approaches are the three types of model based methodologies. At first the principles equations is\are created based on processes like internal electrochemical in electrochemical model-based approaches, and after the correct state is estimated. But, the cost of this strategy is significant, making it difficult to use in online applications. Electric models, such as fractional order circuit equivalent, RC circuit equivalent models are constructed initially in equivalent circuit model-based approaches. The model parameters are then updated using filtering techniques for SOH estimation. Because of its minimal computing cost, this approach may be employed online. In the estimate of battery SOH, empirical/semiempirical model-based approaches are extensively utilized. These approaches are based on the notion of fitting loss of capacity or increase in the resistance with cycles internally.

Machine Learning (ML) is a kind of data analysis that automates the creation of analytical models. It is predicated on the premise that with minimum human interaction, systems can learn from data, discover patterns, and make judgments or predictions[5]. Support vector machine (SVM)[6] and artificial neural network-based approaches are examples of machine learning (ANN). It is not necessary to have a full understanding in the battery's internal circuitry in this case[7]. When employing these clever algorithms to estimate the SOH, the battery is often treated as a black box. The data-driven technique can estimate SOH using cycle data[8-12] and critical factors impacting battery life, but it requires a thorough knowledge of the relationship between activity and deterioration via physical investigation.

In this research, we look at a data-driven strategy for applying machine learning methods to use the charging status profile of current (I), voltage (V), and temperature of the surface lithion batteries (T)[13-15]. To estimate the SoH utilising input data as current, voltage and temperature. generally feed forward neural networks and convolutional neural networks are utilised[16-22].

## II. FRAME WORK

The suggested framework for predicting the capacity of battery using multiple channel of charging



status profiles which are based on CNN and FNN is shown in Fig. 1. Data pre-processing, training, and estimate are the three processes in this approach. Data cleaning and min-max normalisation are used to eliminate aberrant data in stage one. The data set is then separated into three sections: training, validation, and testing. Finally, the voltage, current, temperature, and capacity values are revised. Second step involves using training the sets and validation of the sets to choose the best model based on the ML techniques of CNN and FNN. In the third step estimation of the capacity of battery and assess the efficacy of suggested approaches using capacity estimating models developed in the previous phase.

**Figure 1** Proposed Frame Work

**A. Charging Profile of Multi-Channel of [V],[ I],[ T] data**

As shown in Fig. 2, the charging profiles of voltage, current, and temperature change significantly as a battery ages; during the charging process, The voltage of an old cell hits 4.2 V sooner than that of a fresh new cell, and current of an aged cell starts to decrease from a constant current earlier than that of a fresh cell. Both of these events take place earlier in the lifespan of an aged cell than they do in the lifetime of a fresh cell. Furthermore, the old cell achieves its maximal temperature before the new cell. Because of the recurring process like charging, resting, and battery discharging, the starts profile like temperature of the initial and last cycles are different. Because the temperature increases towards the conclusion of discharging compared to the beginning, the starting temperature of the following charging profile is affected. To effectively assess battery ageing, we must first define the SoH. Despite the fact that there is no universal definition of SoH, it is often defined in terms of capacity as stated by.

$$\text{SoH} (\%) = (C_k / C_0) \times 100 \quad (1)$$

Measured capacity of cycle k is given by  $C_k$ , while  $C_0$  is the rated capacity. Furthermore, we find that battery life is finished when the measured capacity falls below 70% of the specified capacity, indicating that dependable functioning is no longer possible.

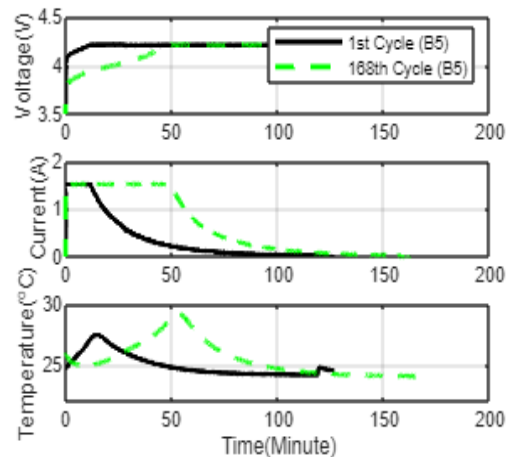


**Figure 2** Charging profile of battery #5 in terms of voltage, current, and temperature for both new cells and older cells from the NASA battery data collection

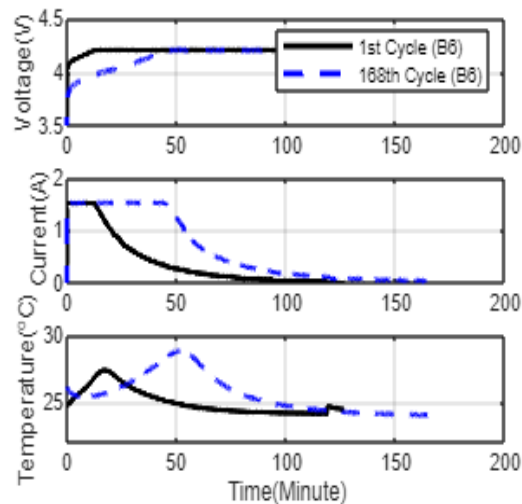


**Figure 3.** charging profile of battery #6 in terms of voltage, current, and temperature for both new cells and older cells from the NASA battery data collection

**B. Data Processing Step**

**1) Data Acquisition**

The deterioration of Li-ion batteries is caused by a variety of causes, and the decline is nonlinear and complicated. To incorporate into a machine learning model that accurately predicts the level of charge of Li-ion batteries, precision and

reliable battery ageing data are required. Conducting battery ageing testing is a time-consuming and difficult procedure. As a result, numerous academics have evaluated their suggested prediction algorithms using publicly accessible battery information. The high-quality publicly accessible NASA Ames Prognostics Centre of Excellence dataset was used in this study based on past research expertise.

The data-sets include lithium batteries of eight that were put across three distinct operating profiles at room temperature, including charging, discharging, and resting. Repeated use of battery charging and discharging cycles on 18650 lithium batteries which are available commercially are used in the research to achieve accelerated ageing. The constant current constant voltage (CCCV) concept is used to charge batteries, which involves charging at 1.5 A constant current till voltage hits cell top limit voltage of 4.2 V, after applying the constant voltage till current decreases to 20 mA. Discharging is carried out at a steady current of 2 A till the voltage of cell reaches 2.7V, 2.5V, and 2.2V, respectively, for batteries #5, #6, and #7. The tests are carried out till the batteries capacity degrades up to 30% of their rated capacity, or 1.4 Ah. This dataset also contains additional electrochemical impedance data, which we did not utilise in our research.

### 2) Data Cleaning

The pre-process of the data is by eliminating outliers and then securing the accessible data before using the battery data set as experimental data. As illustrated in Fig. 4, we eventually get four sets of battery data with deterioration characteristics each cycle; batteries #5, #6, #7, and #18 are selected for the experiment. Table 1 summarises the battery's general specifications and charging/discharging circumstances

**Table 1. Detailed description of the battery used in the NASA prognostics Centre of Excellence data repository**

Battery no	Charging			Discharging	
	Constant current (A)	Upper voltage limit (V)	Cut-off current (mA)	Constant current (A)	Cut-off voltage (V)
Battery #5	1.5	4.2	20	2	2.7
Battery #6	1.5	4.2	20	2	2.5
Battery #7	1.5	4.2	20	2	2.2
Battery #18	1.5	4.2	20	2	2.5

In the meanwhile, despite the fact that there are numerous data points during the charging process that are determined by the BMS [11] settings, it is not possible to utilise all of them due to the data's sensitivity as well as the complexity of the estimation process., therefore we employ FIGURE 3. During the cycle, capacity degrades. data that has been subsampled to preserve and keep the changes throughout the charging period. In order to produce

the proposed models, a uniform sample of the raw battery data was performed first. The retrieved attributes were then utilised as inputs in the models. The input matrix is produced as vectors of 30 dimension by concatenating the V, I, and T charging profiles, each of which includes 10 samples. Each of these charging profiles is represented by a vector. samples number is set to take into account the various variations in time as well as the model's complexity. In addition, to avoid oscillation in small time intervals, we average the data across sampling intervals[12].

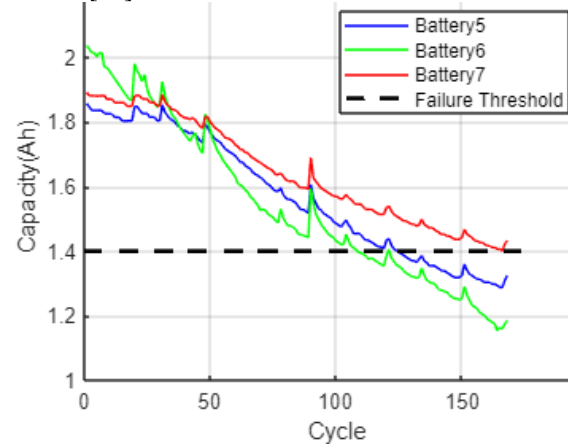


**Figure 4 Degradation of capacity in cycle**

### 3) Normalisation

Min-max normalisation, which maintains the original data distribution with the exception of a factor like scaling and translates the given data in the range of [0,1] as seen below, is the method that we use for more effective training. [23].

$$z_i^k = \frac{y_i^k - \min(y)}{\max(y) - \min(y)} \quad i \in \{1, 2, \dots, n-1, n\} \quad (2)$$

Where  $y$  is the charging cycle total number, represented as  $y^k$ , and  $n$  represents the samples number that are taken during the each cycles. Denormalization will, of course, play a role in the presentation of the estimation findings in final.

### C. Feed-Forward Neural Network (FNN)

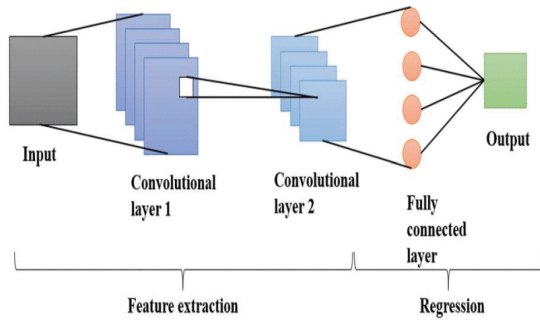
Starting with a feedforward neural network, it is a prominent ML learning technique that does not include feedback connections, we begin our analysis.. Each layer of the FNN contains neurons that provide nonlinear activation based on the connections like weighted to the preceding layer. here utilization of a standard FNN method, with one hidden layer that accounts for input data unpredictability.

#### D. Convolutional Neural Network (CNN)

CNN is a popular architecture in machine learning that employs convolutionary multiplication rather than standard multiplication of matrix in at minimum one of its layers. following is the procedure for 2-dimensional convolution:

$$S(i, j) = (Y * W)(i, j) = \sum_m \sum_n Y(i - m, j - n) W(m, n) \quad (3)$$

The first layer of a convolutional network is referred to as the convolutional layer. The fully-connected layer is the last layer, despite the fact that more convolutional layers or pooling layers might be added after the convolutional layers[13]. The CNN becomes progressively more difficult with each additional layer, which enables it to identify bigger portions of the image. The earlier layers provide an emphasis on fundamental components such as colours and borders. As the visual data moves through the



various levels of the CNN, it starts to differentiate the item's larger components or characteristics, and finally it recognises the object that is the focus of its attention.

Figure 5 Convolution Neural Network

#### E. Validation

The standard training session lasts less than 20 seconds on average, and there is a drop-out rate of half for regularisation. Here the mean squared error is used as a loss function. Both the number of training epochs and the batch size are configurable; currently, they are both set at 500. Leaky ReLU is used for the activation function in this circuit. When it comes to determining how accurate our estimates are, we make use of a standard error index known as the mean absolute percentage error (MAPE).:

$$MAPE(\%) = \frac{100}{K} \sum_{k=1}^K \frac{|l(k) - \hat{l}(k)|}{l(k)} \quad (4)$$

where real capacity is denoted by  $l(k)$ , estimated capacity is denoted by  $\hat{l}(k)$ , and the number of cycles represented by  $K$ . In addition, the following formula is used to get the mean absolute error (MAE) and the root mean square error (RMSE):

### III. RESULT AND DISSCUSSION

FFNN and CNN are used in the process of estimating capacity by using data like current, voltage, and temperature of multiple channel charging profiles with ten data points which are sampled uniformly for each channel.. After estimating the capacity the SOH of lithium ion battery is also calculated. Both approaches' capacity estimates are displayed each cycle in Fig. 6 and Fig. 7, respectively. Fig. 6 shows capacity estimation by both approaches of battery 5 and fig. 7 shows both the approaches of battery 6.

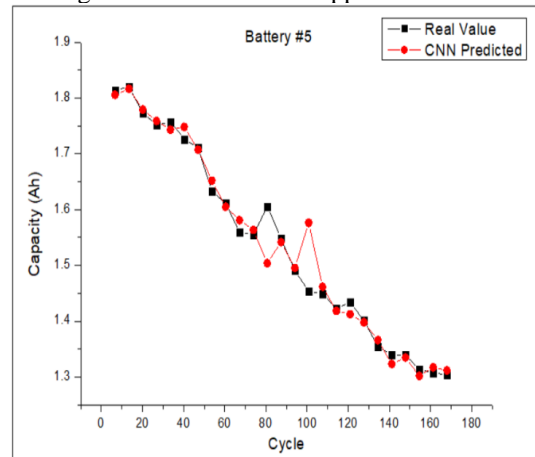


Figure 6.1 capacity estimation of battery #5 using FNN

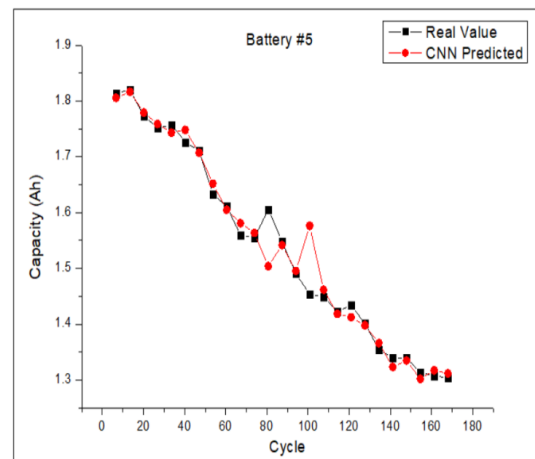


Figure 6.2 capacity estimation of battery #5 using CNN

For batteries 5,6,7, capacity is approximated and observed for both FFNN and CNN. When compared to FFNN, CNN machine learning approaches perform much better. The RMSE of FFNN is greater than that of CNN, as seen in the table. Because CNN has numerous convolution layers, it performs better.

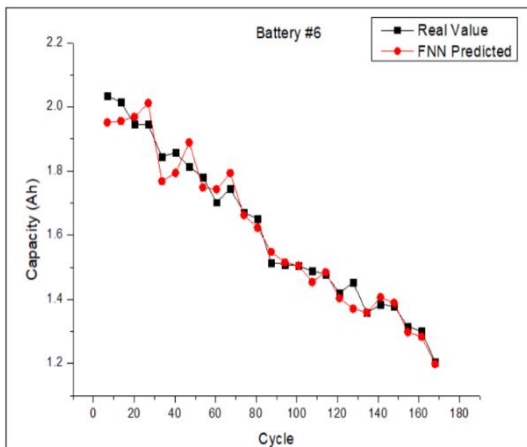


Figure 6.1 capacity estimation of battery #6 using FNN

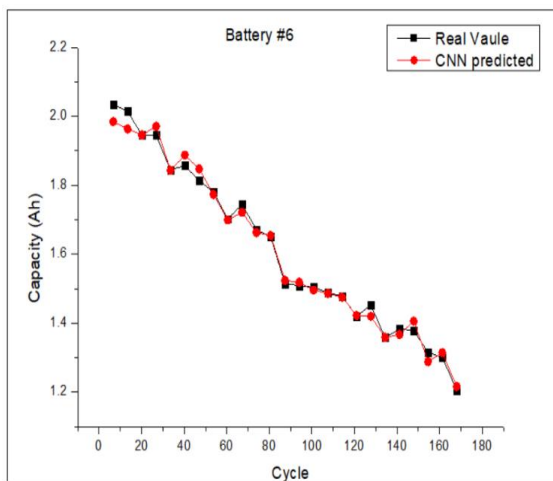


Figure 7.2 capacity estimation of battery #6 using CNN

The SOH of the battery 5 of both the method is shown in fig 8. Fig 8.1 shows the SOH of battery 5 calculated using FNN method and fig 8.2 shows the SOH of battery 5 calculated using CNN method. The SOH of the battery 6 of both the method is shown in fig 9. Fig 9.1 shows the SOH of battery 6 calculated using FNN method and fig 9.2 shows the SOH of battery 6 calculated using CNN method

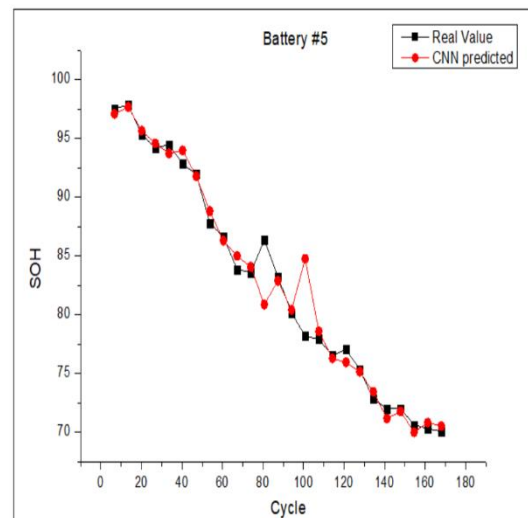
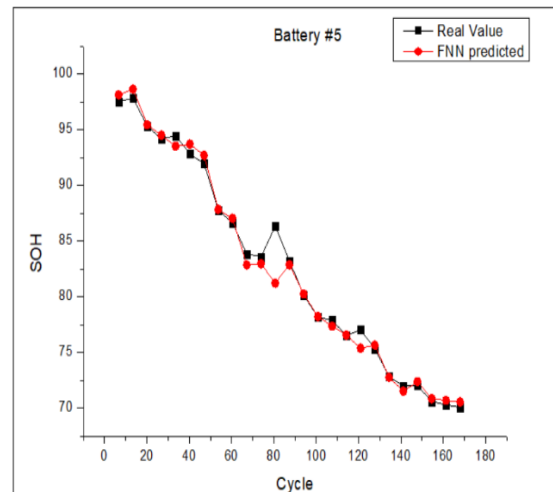
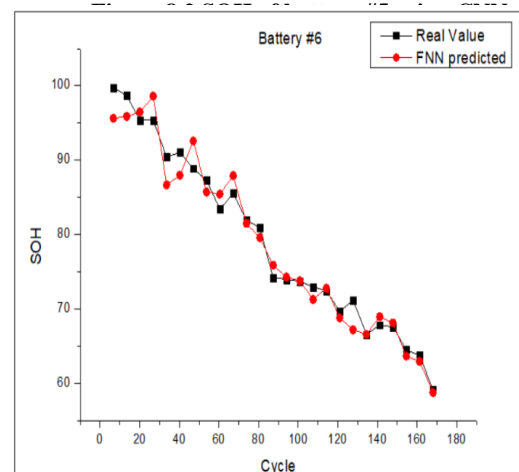


Figure 7.1 SOH of battery #5 using FNN



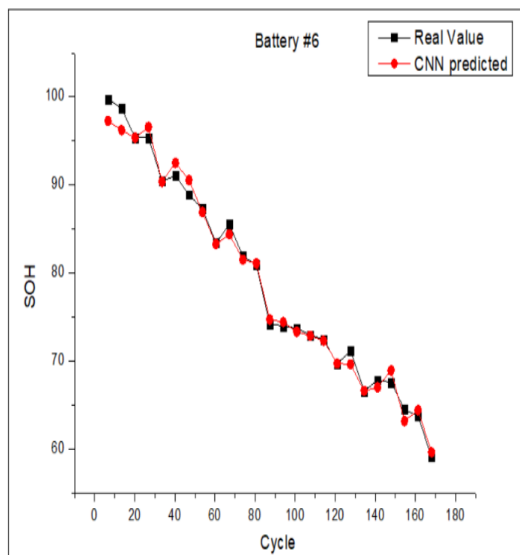


Figure 8.1 SOH of battery #6 using FNN

Figure 9.2 SOH of battery #6 using CNN

#### IV. CONCLUSION

This study discusses a capacity estimate method for lithium batteries that uses FFNN and CNN with multiple channel T, I, and V data to calculate SOH. We investigated the estimate findings of the standpoint of error and differences in capacity each cycle using NASA's lithium-ion battery dataset. The variety of possible data is crucial for high-accuracy estimate, according to numerical findings. CNN outperforms FFNN across the board in all batteries

#### V. REFERENCES

1. M. A. Hannan, M. M. Hoque, A. Hussain, Y. Yusof and P. J. Ker, "State-of-the-Art and Energy Management System of Lithium-Ion Batteries in Electric Vehicle Applications: Issues and Recommendations," in *IEEE Access*, vol. 6, pp. 19362-19378, 2018, doi: 10.1109/ACCESS.2018.2817655.
2. P. Jategaonkar, D. B. Talange, N. C. Amancharla and G. K. Jha, "SOH Algorithm Development of Li-ion Battery Cell for Electric and Hybrid Applications," 2019 International Conference on Power Electronics Applications and Technology in Present Energy Scenario (PETPES), 2019, pp. 1-6, doi: 10.1109/PETPES47060.2019.9003969.
3. R. Ramachandran, D. Ganeshaperumal and B. Subathra, "Parameter Estimation of Battery Pack in EV using Extended Kalman Filters," 2019 IEEE International Conference on Clean Energy and Energy Efficient Electronics Circuit for

- Sustainable Development (INCCES), 2019, pp. 1-5, doi: 10.1109/INCCES47820.2019.9167740.
4. Y. Jiang, J. Zhang, L. Xia and Y. Liu, "State of Health Estimation for Lithium-Ion Battery Using Empirical Degradation and Error Compensation Models," in *IEEE Access*, vol. 8, pp. 123858-123868, 2020, doi: 10.1109/ACCESS.2020.3005229.
5. C. Vidal, P. Malysz, P. Kollmeyer and A. Emadi, "Machine Learning Applied to Electrified Vehicle Battery State of Charge and State of Health Estimation: State-of-the-Art," in *IEEE Access*, vol. 8, pp. 52796-52814, 2020, doi: 10.1109/ACCESS.2020.2980961.
6. C. Weng, J. Sun and H. Peng, "Model Parametrization and Adaptation Based on the Invariance of Support Vectors With Applications to Battery State-of-Health Monitoring," in *IEEE Transactions on Vehicular Technology*, vol. 64, no. 9, pp. 3908-3917, Sept. 2015, doi: 10.1109/TVT.2014.2364554.
7. X. Han et al., "A review on the key issues of the lithium ion battery degradation among the whole life cycle," *eTransportation*, vol. 1, p.100005, 2019/08/01/ 2019, doi:https://doi.org/10.1016/j.etrans.2019.100005.
8. J. Guo, J. Yang, Z. Lin, C. Serrano, and A. M. Cortes, "Impact Analysis of V2G Services on EV Battery Degradation -A Review," in 2019 IEEE Milan PowerTech, 23-27 June 2019 2019, pp. 1-6, doi: 10.1109/PTC.2019.8810982.
9. A. J. Smith, H. M. Dahn, J. C. Burns, and J. R. Dahn, "Long-Term Low-Rate Cycling of LiCoO<sub>2</sub>/Graphite Li-Ion Cells at 55°C," *Journal of The Electrochemical Society*, vol. 159, no. 6, pp. A705- A710, 2012, doi: 10.1149/2.056206jes.
10. P. Keil et al., "Calendar Aging of Lithium-Ion Batteries," *Journal of The Electrochemical Society*, vol. 163, no. 9, pp. A1872-A1880, 2016, doi: 10.1149/2.0411609jes.
11. K. Liu, T. R. Ashwin, X. Hu, M. Lucu, and W. D. Widanage, "An evaluation study of different modelling techniques for calendar ageing prediction of lithium-ion batteries," *Renewable and Sustainable Energy Reviews*, vol. 131, p. 110017, 2020/10/01/ 2020, doi: https://doi.org/10.1016/j.rser.2020.110017.
12. H. Farzin, M. Fotuhi-Firuzabad, and M. Moeini-Aghtaie, "A Practical Scheme to Involve Degradation Cost of Lithium-Ion Batteries in Vehicle-to-Grid Applications," *IEEE Transactions on Sustainable Energy*, vol. 7, no. 4,

- pp. 1730-1738, 2016, doi:10.1109/TSTE.2016.2558500.
13. K. Ginigeme and Z. Wang, "Distributed Optimal Vehicle-To-Grid Approaches With Consideration of Battery Degradation Cost Under Real-Time Pricing," *IEEE Access*, vol. 8, pp. 5225-5235, 2020, doi:10.1109/ACCESS.2019.2963692.
  14. S. Amama and J. Marco, "Vehicle-to-Grid Aggregator to Support Power Grid and Reduce Electric Vehicle Charging Cost," *IEEE Access*, vol. 7, pp. 178528-178538, 2019, doi:10.1109/ACCESS.2019.2958664.
  15. K. Uddin, M. Dubarry, and M. B. Glick, "The viability of vehicle-to-grid operations from a battery technology and policy perspective," *Energy Policy*, vol. 113, pp. 342-347, 2018/02/01/2018, doi: <https://doi.org/10.1016/j.enpol.2017.11.015>.
  16. Y. Yu, O. S. Nduka, and B. C. Pal, "Smart Control of an Electric Vehicle for Ancillary Service in DC Microgrid," *IEEE Access*, vol. 8, pp. 197222-197235, 2020, doi: 10.1109/ACCESS.2020.3034496.
  17. A. Marongiu, M. Roscher, and D. U. Sauer, "Influence of the vehicle-to-grid strategy on the aging behavior of lithium battery electric vehicles," *Applied Energy*, vol. 137, pp. 899-912, 2015/01/01/ 2015, doi: <https://doi.org/10.1016/j.apenergy.2014.06.063>.
  18. J. de Hoog et al., "Combined cycling and calendar capacity fade modeling of a Nickel-Manganese-Cobalt Oxide Cell with real-life profile validation," *Applied Energy*, vol. 200, pp. 47-61, 2017/08/15/ 2017, doi: <https://doi.org/10.1016/j.apenergy.2017.05.018>.
  19. E. Redondo-Iglesias, P. Venet, and S. Pelissier, "Modelling Lithium-Ion Battery Ageing in Electric Vehicle Applications—Calendar and Cycling Ageing Combination Effects," *Batteries*, vol. 6, no. 1, 2020, doi: 10.3390/batteries6010014.
  20. G. Zhang, S. T. Tan, and G. G. Wang, "Real-Time Smart Charging of Electric Vehicles for Demand Charge Reduction at Non-Residential Sites," *IEEE Transactions on Smart Grid*, vol. 9, no. 5, pp. 4027-4037, 2018, doi: 10.1109/TSG.2016.2647620.
  21. N. I. Nimalsiri, C. P. Mediwaththe, E. L. Ratnam, M. Shaw, D. B. Smith, and S. K. Halgamuge, "A Survey of Algorithms for Distributed Charging Control of Electric Vehicles in Smart Grid," *IEEE Transactions on Intelligent Transportation Systems*, pp. 1-19, 2019, doi: 10.1109/TITS.2019.2943620.
  22. J. D. K. Bishop, C. J. Axon, D. Bonilla, M. Tran, D. Banister, and M. D. McCulloch, "Evaluating the impact of V2G services on the degradation of batteries in PHEV and EV," *Applied Energy*, vol. 111, pp. 206-218, 2013/11/01/ 2013, doi: <https://doi.org/10.1016/j.apenergy.2013.04.094>.